

## Patterning of Robust Self-Assembled n-type Hexaazatrinaphthylene-Based Nanorods and Nanowires by Microcontact Printing

Hin-Lap Yip,<sup>†</sup> Jingyu Zou,<sup>†,§</sup> Hong Ma,<sup>†</sup> Yanqing Tian,<sup>†</sup> Neil M. Tucker,<sup>‡</sup> and Alex K.-Y. Jen<sup>\*,†,‡</sup>

Department of Materials Science and Engineering and Department of Chemistry, University of Washington, Seattle, Washington 98195, and Department of Materials Science, Sichuan University, Chengdu 610064, People's Republic of China

Received July 11, 2006; E-mail: ajen@u.washington.edu.

The fabrication of functional nanostructures using self-assembled one-dimensional (1-D)  $\pi$ -conjugated molecules represents a new method to create devices with single-crystal-like properties. This approach has been proposed as an alternative for carbon nanotubes and inorganic wires-based nanoscale optoelectronic devices.<sup>1</sup> However, there are still several important hurdles that need to be addressed in order to use these materials in active devices. These challenges include a better control of the dimension of the nanostructures and structural robustness of these materials for processing and patterning on surfaces. So far, most of the supramolecular nanowires reported in the literature are based on p-type  $\pi$ -conjugated materials, and it is essential to develop complementary n-type nanowires for fabricating complete functional devices.<sup>1c</sup>

Here we report the self-assembling properties of alkylamide-tethered hexaazatrinaphthylenes (HATNA) as the first step toward this direction. The structures of molecules **1** and **2** studied are illustrated in Figure 1. HATNA is an electron-deficient discotic  $\pi$ -conjugated molecule that possesses n-type transporting characteristics. It has a  $C_{3h}$  symmetry with well-defined *face-to-face* columnar packing in its crystal structure.<sup>2a</sup> HATNA-based materials have also been theoretically<sup>2b</sup> and experimentally<sup>2c-d</sup> proven to have high charge mobility. Compound **1** has good solubility in  $\text{CHCl}_3$ ; however, it gels easily in mixed solvents such as  $\text{CHCl}_3$ /hexane (*v/v* = 1:1) owing to enhanced amide–amide hydrogen bonding in a less polar environment, which is one of the main driving forces for the formation of supramolecular nanofibers.<sup>3</sup> The morphological study reveals that **1** forms self-organized nanowires with a diameter of  $\sim 20$  nm and a length over  $10 \mu\text{m}$  in the gel (see Supporting Information).

To create shape-persistent nanostructures, the fixation of supramolecular nanowires through chemical or photochemical reaction-induced cross-linking or polymerization at their self-assembled state have been demonstrated.<sup>4</sup> In our study, a similar approach was applied to compound **2** which possesses diacetylene groups that can be converted into polydiacetylene via photopolymerization to create robust nanostructures. The self-assembling properties of **2** are very different from those of **1** in  $\text{CHCl}_3$ . The introduction of  $\pi$ -conjugated diacetylene groups further enhances the  $\pi$ – $\pi$  stacking between the molecules. The shortened flexible alkyl groups also reduce the solvation of the molecules in  $\text{CHCl}_3$ . As a result, the binding force between the molecules increases, and these molecules start to aggregate at a lower concentration ( $\sim 1 \times 10^{-5}$  M in  $\text{CHCl}_3$ ). The absorption spectrum of **2** in  $\text{CHCl}_3$  shows three characteristic peaks at 407, 386, and 306 nm (Figure 2). The first two peaks correspond to the transitions between the 0–0 and 0–1 states,<sup>5</sup> respectively, and the main peak corresponds to the transition to a higher level. By increasing the concentration from  $2 \times 10^{-6}$  to  $1 \times 10^{-4}$  M, all peaks decrease in absorbance. The ratio between the 0–0 and the 0–1 transitions decreases from 1.12 to 0.97, and the main peak

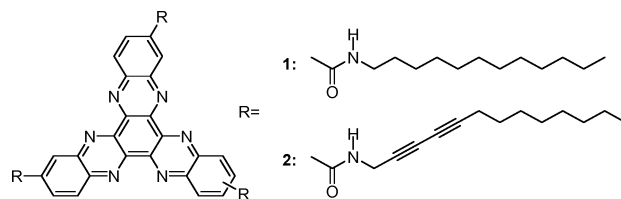


**Figure 1.** Structure of HATNAs. Compound **1** and **2** are tethered with an amide-dodecyl group and an amide-diacetylene-octanyl group, respectively.

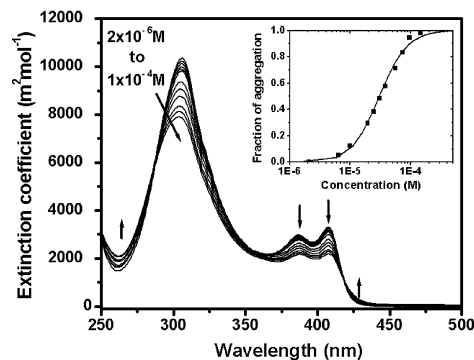


**Figure 2.** Concentration-dependent UV–vis spectra from compound **2** in  $\text{CHCl}_3$  at room temperature. The inset shows the fraction of aggregation as a function of concentration of **2** in  $\text{CHCl}_3$ .

absorbance also hypsochromically shifted 4 nm from 306 to 302 nm which indicates the formation of H-aggregates.<sup>5</sup> By fitting the spectroscopic data using the isodesmic (or equal  $K$ ) model,<sup>6</sup> a plot of fraction of aggregation ( $\alpha_{\text{aggr}}$ ) as a function of concentration can be established. The calculated average binding constant  $K$  for **2** (in  $\text{CHCl}_3$ ) from three different wavelengths is  $8 \times 10^3 \text{ M}^{-1}$ .

Controlling the dimension of self-assembled nanostructure in solid-state is essential for further integration of these functional materials into a miniaturized device. Guided by the plot of  $\alpha_{\text{aggr}}$  versus concentration in Figure 2, we can correlate the solid-state organization of **2** with their self-assembled states in solution through a morphological study of the nanostructures deposited from their corresponding aggregates in solution. The AFM images in Figure 3 show an increase in the columnar stack length with concentration, while the stack diameters in all cases remain unchanged. When molecule **2** was deposited from solutions with low  $\alpha_{\text{aggr}}$  (Figure 3a–c), nanorod structures with tunable lengths could be obtained. At high  $\alpha_{\text{aggr}}$  (Figure 3d), nanowires with length over  $10 \mu\text{m}$  were formed.

The photo-cross-linking of the diacetylene units in **2** was conducted by exposing the self-assembled nanowires to an 18 W UV lamp in both solid and solution phase. For photo cross-linking in solid phase, the nanowires were drop cast from a  $1 \times 10^{-4}$  M  $\text{CHCl}_3$  solution onto a quartz substrate, and the process was monitored by the time-dependent UV–vis absorption spectrum. The appearance of the absorption peaks at 590 and 536 nm in Figure 4a correspond to the formation of polydiacetylene.<sup>7</sup> Polymerization

<sup>†</sup> Department of Materials Science and Engineering, University of Washington.

<sup>‡</sup> Department of Chemistry, University of Washington.

<sup>§</sup> Department of Materials Science, Sichuan University.

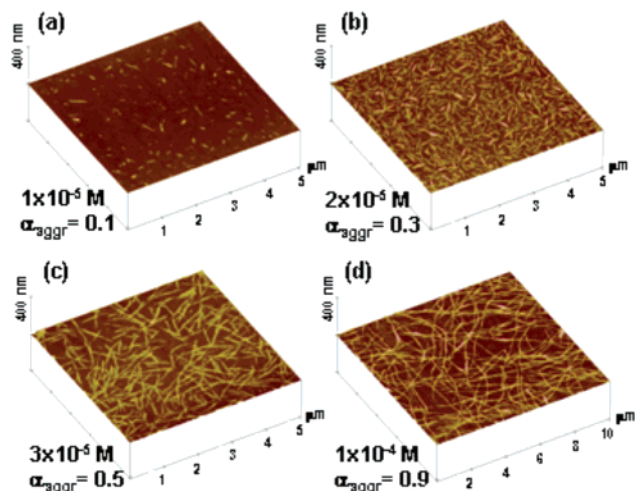


**Figure 3.** AFM images of **2** spin-coated on SiO<sub>2</sub>/Si substrates from different concentrations in CHCl<sub>3</sub>. The spin speed in all cases was fixed at 3000 rpm. The observed lengths of the 1-D nanostructures based on the AFM result are (a) 50–250 nm, (b) 300–500 nm, (c) 1–1.5 μm, and (d) over 10 μm. The thickness of the nanostructure in all cases is between 2–5 nm, which corresponds to columnar stacks with only 1–2 molecular thickness.

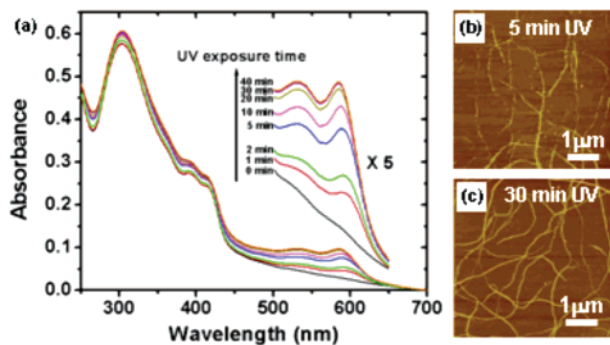


**Figure 4.** (a) Time dependence of UV–vis spectral change of **2** upon UV irradiation. AFM images of **2** after (b) 5 min and (c) 30 min UV irradiation followed by 3 min of CHCl<sub>3</sub> rinsing. The nanowires were prepared by spin casting the  $1 \times 10^{-4}$  M of **2** in CHCl<sub>3</sub> solution on SiO<sub>2</sub>/Si substrates.

was completed after 30 min of UV irradiation, and no further increase in polydiacetylene absorption was noticeable after longer UV exposure. The robustness of the resulting cross-linked nanowires is evident against solvent washing as shown in the AFM images (Figure 4b,c). After UV curing for 5 min, a substantial amount of nanowires can still be washed away after rinsing with CHCl<sub>3</sub>, and the nanowire structure was also destroyed (Figure 4b). On the contrary, there is no apparent loss from the heavily cross-linked nanowires (Figure 4c). Nevertheless, photo-cross-linking of nanowires in solution resulted in break down of the nanowires into shorter segments because of structural perturbation during polymerization (see Supporting Information).

Since surface patterning of 1-D nanomaterials such as carbon nanotubes<sup>8a,b</sup> and inorganic nanowires<sup>8c</sup> is a critical element for fabricating nanoscale functional devices, we have also explored the feasibility of creating robust patterns using these self-assembled nanowires. We have employed the microcontact printing ( $\mu$ CP) technique to form patterns of nanowires and nanorods of **2**. The self-assembled nanostructures were first spin-coated onto a patterned PDMS stamp, which was then allowed to form conformal contact with a SiO<sub>2</sub>/Si substrate for 30 s to transfer the nanostructures to the surface. These nanostructures could be directly transferred to SiO<sub>2</sub>/Si substrate without the need of any surface modification, and they formed robust patterns after postpolymerization by UV treatment (Figure 5).

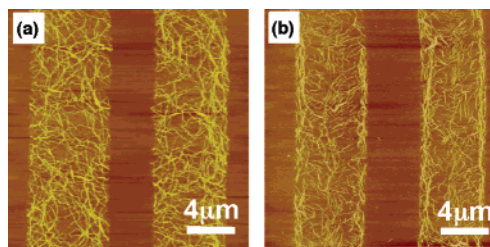


**Figure 5.** AFM images of (a) nanowires and (b) nanorods pattern of **2** on SiO<sub>2</sub>/Si fabricated by  $\mu$ CP. Images were taken after 30 min UV treatment followed by 3 min CHCl<sub>3</sub> rinsing. The nanowires ( $1 \times 10^{-4}$  M in CHCl<sub>3</sub>) and nanorods ( $3 \times 10^{-5}$  M in CHCl<sub>3</sub>) were spin-coated on PDMS stamps with  $6 \mu\text{m} \times 4 \mu\text{m}$  line pattern at 3000 rpm.

In summary, structurally robust columnar stacks of n-type  $\pi$ -conjugated molecules with tunable lengths can be obtained by utilizing postpolymerization techniques after forming the supramolecular self-assembly initially. These nanostructures can be easily transferred to the substrate surface to create desired patterns by microcontact printing. We believe that this simple patterning method should be generally applicable to other 1-D self-assembled nanostructures for fabricating devices based on functional supramolecular materials.

**Acknowledgment.** This work was supported by the Air Force Office of Scientific Research (AFOSR) under the Bio-inspired Concept Program. A. K.-Y. Jen thanks the Boeing-Johnson Foundation for financial support. H.-L. Yip thanks the Nanotechnology Fellowship sponsored by the University Initiative Fund (UIF) at the University of Washington.

**Note Added after ASAP Publication.** There was an error in the spelling of an author's name in the version published ASAP September 16, 2006. The corrected version was published ASAP September 20, 2006.

**Supporting Information Available:** Details of synthesis and characterization of **1** and **2**, experimental details, AFM study of **1**, IR, UV–vis and AFM study of **2** before and after photopolymerization in solid and solution phases. This material is available free of charge via the Internet at <http://pubs.acs.org>.

## References

- (1) (a) Meijer, E. W.; Schenning, A. P. H. *J. Nature* **2002**, *419*, 353–354. (b) Hoeben, F. J. M.; Jonkheijm, P.; Meijer, E. W.; Schenning, A. P. H. *J. Chem. Rev.* **2005**, *105*, 1491–1546. (c) Schenning, A. P. H. J.; Meijer, E. W. *Chem. Comm.* **2005**, *26*, 3245–3258. (d) Hill, J. P.; Jin, W.; Kosaka, A.; Fukushima, T.; Ichihara, H.; Shimomura, T.; Ito, K.; Hashizume, T.; Ishii, N.; Aida, T. *Science* **2004**, *304*, 1481–1483.
- (2) (a) Du, M.; Bu, X. H.; Biradha, K. *Acta Cryst.* **2001**, *C57*, 199–200. (b) Lemaur, V.; da Silva Filho, D. A.; Coropceanu, V.; Lehmann, M.; Geerts, Y.; Piris, J.; Debije, M. G.; van de Craats, A. M.; Senthilkumar, K.; Siebbeles, L. D. A.; Warman, J. M.; Bredas, J.-L.; Cornil, J. *J. Am. Chem. Soc.* **2004**, *126*, 3271–3279. (c) Lehmann, M.; Kestemont, G.; Aspe, R. G.; Buess-Herman, C.; Koch, M. H. J.; Debije, M. G.; Piris, J.; de Hass, M. P.; Warman, J. M.; Watson, M. D.; Lemaur, V.; Cornil, J.; Geerts, Y. H.; Gearba, R.; Ivanov, D. A. *Chem.–Eur. J.* **2005**, *11*, 3349–3362. (d) Kaafarani, B. R.; Kondo, T.; Yu, J.; Zhang, Q.; Dattilo, D.; Risko, C.; Jones, S. C.; Barlow, S.; Domercq, B.; Amy, F.; Kahn, A.; Bredas, J. L.; Kippelen, B.; Marder, S. R. *J. Am. Chem. Soc.* **2005**, *127*, 16358–16359.
- (3) Ornatka, M.; Peleshanko, S.; Genson, K. L.; Rybak, B.; Bergman, K. N.; Tsukruk, V. V. *J. Am. Chem. Soc.* **2004**, *126*, 9675–9684.
- (4) (a) Chang, J. Y.; Baik, J. H.; Lee, C. B.; Han, M. J. *J. Am. Chem. Soc.* **1997**, *119*, 3197–3198. (b) Shirakawa, M.; Fujita, N.; Shinkai, S. *J. Am. Chem. Soc.* **2005**, *127*, 4164–4165. (c) Masuda, M.; Jonkheijm, P.; Sijbesma, R. P.; Meijer, E. W. *J. Am. Chem. Soc.* **2003**, *125*, 15935–15940. (d) Jin, W.; Fukushima, T.; Kosaka, A.; Miki, M.; Ishii, N.; Aida, T. *J. Am. Chem. Soc.* **2005**, *127*, 8284–8285.
- (5) Ishi-I, T.; Yaguma, K.; Kuwahara, R.; Taguri, Y.; Mataka, S. *Org. Lett.* **2006**, *8*, 585–588.
- (6) Martin, R. B. *Chem. Rev.* **1996**, *96*, 3043–3064.
- (7) Okada, S.; Peng, S.; Spevak, W.; Charych, D. *Acc. Chem. Res.* **1998**, *31*, 229–239.
- (8) (a) Tsukruk, V. V.; Ko, H.; Peleshanko, S. *Phys. Rev. Lett.* **2004**, *92*, 065502. (b) Meitl, M. A.; Zhou, Y.; Gaur, A.; Jeon, S.; Usrey, M. L.; Strano, M. S.; Rogers, J. A. *Nano Lett.* **2004**, *4*, 1643–1647. (c) Huang, Y.; Duan, X.; Wei, Q.; Leiber, C. M. *Science* **2001**, *291*, 630–633.

JA064934K